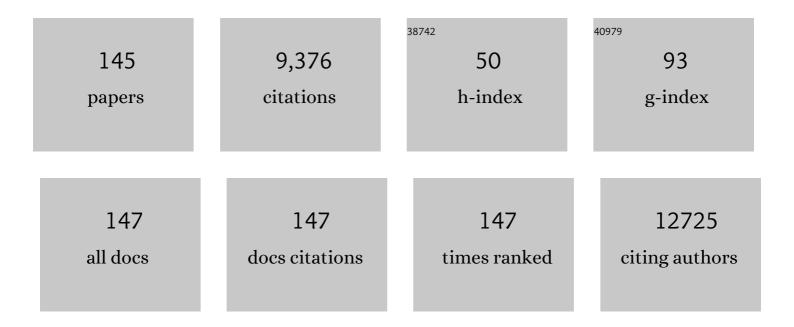
Juan Antonio Zapien

List of Publications by Year in descending order

Source: https://exaly.com/author-pdf/7865618/publications.pdf Version: 2024-02-01



| # | Article | IF | CITATIONS |
|----|---|-------|-----------|
| 1 | High-Density, Ordered Ultraviolet Light-Emitting ZnO Nanowire Arrays. Advanced Materials, 2003, 15, 838-841. | 21.0 | 598 |
| 2 | Initiating a mild aqueous electrolyte Co ₃ O ₄ /Zn battery with 2.2 V-high voltage and 5000-cycle lifespan by a Co(<scp>iii</scp>) rich-electrode. Energy and Environmental Science, 2018, 11, 2521-2530. | 30.8 | 414 |
| 3 | Hydrogenâ€Free and Dendriteâ€Free Allâ€Solidâ€State Znâ€Ion Batteries. Advanced Materials, 2020, 32, e19081 | 221.0 | 381 |
| 4 | Achieving Highâ€Voltage and Highâ€Capacity Aqueous Rechargeable Zinc Ion Battery by Incorporating Twoâ€Species Redox Reaction. Advanced Energy Materials, 2019, 9, 1902446. | 19.5 | 341 |
| 5 | Single-Site Active Iron-Based Bifunctional Oxygen Catalyst for a Compressible and Rechargeable Zinc–Air Battery. ACS Nano, 2018, 12, 1949-1958. | 14.6 | 336 |
| 6 | Superâ€Stretchable Zinc–Air Batteries Based on an Alkalineâ€Tolerant Dualâ€Network Hydrogel Electrolyte. Advanced Energy Materials, 2019, 9, 1803046. | 19.5 | 287 |
| 7 | Well-Aligned ZnO Nanowire Arrays Fabricated on Silicon Substrates. Advanced Functional Materials, 2004, 14, 589-594. | 14.9 | 272 |
| 8 | Silicon nanowires-based highly-efficient SERS-active platform for ultrasensitive DNA detection. Nano Today, 2011, 6, 122-130. | 11.9 | 257 |
| 9 | Flexible Waterproof Rechargeable Hybrid Zinc Batteries Initiated by Multifunctional Oxygen Vacancies-Rich Cobalt Oxide. ACS Nano, 2018, 12, 8597-8605. | 14.6 | 257 |
| 10 | A flexible solid-state zinc ion hybrid supercapacitor based on co-polymer derived hollow carbon spheres. Journal of Materials Chemistry A, 2019, 7, 7784-7790. | 10.3 | 254 |
| 11 | p-Type ZnO Nanowire Arrays. Nano Letters, 2008, 8, 2591-2597. | 9.1 | 237 |
| 12 | Wavelength-Controlled Lasing in ZnxCd1-xS Single-Crystal Nanoribbons. Advanced Materials, 2005, 17, 1372-1377. | 21.0 | 203 |
| 13 | ZnO/Au Composite Nanoarrays As Substrates for Surface-Enhanced Raman Scattering Detection. Journal of Physical Chemistry C, 2010, 114, 93-100. | 3.1 | 190 |
| 14 | Vertically Aligned ZnO Nanorod Arrays Sentisized with Gold Nanoparticles for Schottky Barrier Photovoltaic Cells. Journal of Physical Chemistry C, 2009, 113, 13433-13437. | 3.1 | 174 |
| 15 | A Polyoxometalate-Assisted Electrochemical Method for Silicon Nanostructures Preparation:Â From Quantum Dots to Nanowires. Journal of the American Chemical Society, 2007, 129, 5326-5327. | 13.7 | 163 |
| 16 | Graphitic carbon nitride nanosheet@metal–organic framework core–shell nanoparticles for photo-chemo combination therapy. Nanoscale, 2015, 7, 17299-17305. | 5.6 | 160 |
| 17 | Lasing in ZnS nanowires grown on anodic aluminum oxide templates. Applied Physics Letters, 2004, 85, 2361-2363. | 3.3 | 150 |
| 18 | Surface Engineering of ZnO Nanostructures for Semiconductor‣ensitized Solar Cells. Advanced Materials, 2014, 26, 5337-5367. | 21.0 | 149 |

| # | Article | IF | CITATIONS |
|----|--|------|-----------|
| 19 | Room-temperature single nanoribbon lasers. Applied Physics Letters, 2004, 84, 1189-1191. | 3.3 | 147 |
| 20 | Homoepitaxial Growth and Lasing Properties of ZnS Nanowire and Nanoribbon Arrays. Advanced Materials, 2006, 18, 1527-1532. | 21.0 | 140 |
| 21 | Ruthenium(II) Complex Incorporated UiO-67 Metal–Organic Framework Nanoparticles for Enhanced Two-Photon Fluorescence Imaging and Photodynamic Cancer Therapy. ACS Applied Materials & Interfaces, 2017, 9, 5699-5708. | 8.0 | 129 |
| 22 | A High-Efficiency Surface-Enhanced Raman Scattering Substrate Based on Silicon Nanowires Array Decorated with Silver Nanoparticles. Journal of Physical Chemistry C, 2010, 114, 1969-1975. | 3.1 | 123 |
| 23 | Synthesis, Characterization, and Photocatalytic Application of Different ZnO Nanostructures in Array Configurations. Crystal Growth and Design, 2009, 9, 3222-3227. | 3.0 | 116 |
| 24 | Rapid Microwave Synthesis of Porous TiO ₂ Spheres and Their Applications in Dye-Sensitized Solar Cells. Journal of Physical Chemistry C, 2011, 115, 10419-10425. | 3.1 | 111 |
| 25 | Towards high areal capacitance, rate capability, and tailorable supercapacitors: Co ₃ O ₄ @polypyrrole core–shell nanorod bundle array electrodes. Journal of Materials Chemistry A, 2018, 6, 19058-19065. | 10.3 | 110 |
| 26 | High-quality CdS nanoribbons with lasing cavity. Applied Physics Letters, 2004, 85, 3241-3243. | 3.3 | 109 |
| 27 | Visible–NIR photodetectors based on CdTe nanoribbons. Nanoscale, 2012, 4, 2914. | 5.6 | 99 |
| 28 | Polyhedral Organic Microcrystals: From Cubes to Rhombic Dodecahedra. Angewandte Chemie - International Edition, 2009, 48, 9121-9123. | 13.8 | 97 |
| 29 | Hydrothermal synthesis of ordered single-crystalline rutile TiO2 nanorod arrays on different substrates. Applied Physics Letters, 2010, 96, . | 3.3 | 97 |
| 30 | Effect of the magnetic order on the room-temperature band-gap of Mn-doped ZnO thin films. Applied Physics Letters, 2013, 102, . | 3.3 | 91 |
| 31 | Low-Temperature Synthesis of CulnSe ₂ Nanotube Array on Conducting Glass Substrates for Solar Cell Application. ACS Nano, 2010, 4, 6064-6070. | 14.6 | 86 |
| 32 | Self-assembled three-dimensional mesoporous ZnFe2O4-graphene composites for lithium ion batteries with significantly enhanced rate capability and cycling stability. Journal of Power Sources, 2015, 275, 769-776. | 7.8 | 81 |
| 33 | Uniform Virusâ€Like Co–N–Cs Electrocatalyst Derived from Prussian Blue Analog for Stretchable Fiberâ€Shaped Zn–Air Batteries. Advanced Functional Materials, 2020, 30, 1908945. | 14.9 | 81 |
| 34 | Facile synthesis and electrochemical characterization of porous and dense TiO2 nanospheres for lithium-ion battery applications. Journal of Power Sources, 2011, 196, 6394-6399. | 7.8 | 75 |
| 35 | Light-weight 3D Co–N-doped hollow carbon spheres as efficient electrocatalysts for rechargeable zinc–air batteries. Nanoscale, 2018, 10, 10412-10419. | 5.6 | 73 |
| 36 | Hierarchical self-assembled Bi ₂ S ₃ hollow nanotubes coated with sulfur-doped amorphous carbon as advanced anode materials for lithium ion batteries. Nanoscale, 2018, 10, 13343-13350. | 5.6 | 67 |

| # | Article | IF | CITATIONS |
|----|---|------|-----------|
| 37 | Enhanced electrochemical performance of lithium ion batteries using Sb ₂ S ₃ nanorods wrapped in graphene nanosheets as anode materials. Nanoscale, 2018, 10, 3159-3165. | 5.6 | 65 |
| 38 | Investigation of high performance TiO ₂ nanorod array perovskite solar cells. Journal of Materials Chemistry A, 2017, 5, 15970-15980. | 10.3 | 64 |
| 39 | Facile solution growth of vertically aligned ZnO nanorods sensitized with aqueous CdS and CdSe quantum dots for photovoltaic applications. Nanoscale Research Letters, 2011, 6, 340. | 5.7 | 61 |
| 40 | Enhanced Performance of PTB7:PC ₇₁ BM Solar Cells via Different Morphologies of Gold Nanoparticles. ACS Applied Materials & Interfaces, 2014, 6, 20676-20684. | 8.0 | 61 |
| 41 | Graphene/acid assisted facile synthesis of structure-tuned Fe3O4 and graphene composites as anode materials for lithium ion batteries. Carbon, 2015, 86, 310-317. | 10.3 | 61 |
| 42 | Synthesis of CNT@Fe3O4-C hybrid nanocables as anode materials with enhanced electrochemical performance for lithium ion batteries. Electrochimica Acta, 2015, 176, 1332-1337. | 5.2 | 61 |
| 43 | Raman Spectrum of silicon nanowires. Materials Science and Engineering C, 2003, 23, 931-934. | 7.3 | 60 |
| 44 | Thermal evaporation-induced anhydrous synthesis of Fe3O4–graphene composite with enhanced rate performance and cyclic stability for lithium ion batteries. Physical Chemistry Chemical Physics, 2013, 15, 7174. | 2.8 | 58 |
| 45 | Facile hydrothermal synthesis of CuFeO ₂ hexagonal platelets/rings and graphene composites as anode materials for lithium ion batteries. Chemical Communications, 2014, 50, 10151-10154. | 4.1 | 58 |
| 46 | Facile and Rapid Synthesis of Highly Porous Wirelike TiO ₂ as Anodes for Lithium-Ion Batteries. ACS Applied Materials & Interfaces, 2012, 4, 1608-1613. | 8.0 | 57 |
| 47 | One-pot scalable synthesis of Cu–CuFe ₂ O ₄ /graphene composites as anode materials for lithium-ion batteries with enhanced lithium storage properties. Journal of Materials Chemistry A, 2014, 2, 13892. | 10.3 | 56 |
| 48 | Synthesis of Homogeneously Alloyed Cu _{2â^'<i>x</i>} (S _{<i>y</i>} Se _{1â^'<i>y</i>}) Nanowire Bundles with Tunable Compositions and Bandgaps. Advanced Functional Materials, 2010, 20, 4190-4195. | 14.9 | 55 |
| 49 | Controllable Fabrication of Three-Dimensional Radial ZnO Nanowire/Silicon Microrod Hybrid Architectures. Crystal Growth and Design, 2011, 11, 147-153. | 3.0 | 52 |
| 50 | Theoretical and experimental study of the response of CuO gas sensor under ozone. Sensors and Actuators B: Chemical, 2014, 190, 8-15. | 7.8 | 52 |
| 51 | Polymer-pyrolysis assisted synthesis of vanadium trioxide and carbon nanocomposites as high performance anode materials for lithium-ion batteries. Journal of Power Sources, 2014, 261, 184-187. | 7.8 | 52 |
| 52 | Green and facile synthesis of Fe ₃ O ₄ and graphene nanocomposites with enhanced rate capability and cycling stability for lithium ion batteries. Journal of Materials Chemistry A, 2015, 3, 16206-16212. | 10.3 | 50 |
| 53 | Continuous near-infrared-to-ultraviolet lasing from II-VI nanoribbons. Applied Physics Letters, 2007, 90, 213114. | 3.3 | 49 |
| 54 | Microwave-assisted hydrothermal synthesis of porous SnO2 nanotubes and their lithium ion storage properties. Journal of Solid State Chemistry, 2012, 190, 104-110. | 2.9 | 46 |

| # | Article | IF | CITATIONS |
|----|--|------|-----------|
| 55 | Sodium″on Hybrid Battery Combining an Anion″ntercalation Cathode with an Adsorptionâ€Type Anode for Enhanced Rate and Cycling Performance. Batteries and Supercaps, 2019, 2, 440-447. | 4.7 | 46 |
| 56 | Photoluminescence and photoconductivity properties of copper-doped Cd1â^xZnxS nanoribbons. Nanotechnology, 2006, 17, 5935-5940. | 2.6 | 45 |
| 57 | Wavelength-tunable lasing in single-crystal CdS1â^'XSeX nanoribbons. Nanotechnology, 2007, 18, 365606. | 2.6 | 45 |
| 58 | Facile Synthesis of Hollow Mesoporous CoFe ₂ O ₄ Nanospheres and Graphene Composites as Highâ€Performance Anode Materials for Lithiumâ€Ion Batteries. ChemElectroChem, 2015, 2, 1010-1018. | 3.4 | 45 |
| 59 | Violet-blue LEDs based on p-GaN/n-ZnO nanorods and their stability. Nanotechnology, 2011, 22, 245202. | 2.6 | 43 |
| 60 | Enhanced performance by incorporation of zinc oxide nanowire array for organic-inorganic hybrid solar cells. Applied Physics Letters, 2012, 100, . | 3.3 | 43 |
| 61 | Scalable synthesis of Fe3O4 nanoparticles anchored on graphene as a high-performance anode for lithium ion batteries. Journal of Solid State Chemistry, 2013, 201, 330-337. | 2.9 | 43 |
| 62 | Facile solution synthesis without surfactant assistant for ultra long Alq3 sub-microwires and their enhanced field emission and waveguide properties. Journal of Materials Chemistry, 2010, 20, 3006. | 6.7 | 40 |
| 63 | Nitrogen-Doped Carbon-Encapsulated Antimony Sulfide Nanowires Enable High Rate Capability and Cyclic Stability for Sodium-Ion Batteries. ACS Applied Nano Materials, 2019, 2, 1457-1465. | 5.0 | 40 |
| 64 | Evaporation-induced synthesis of carbon-supported Fe3O4 nanocomposites as anode material for lithium-ion batteries. CrystEngComm, 2013, 15, 1324. | 2.6 | 38 |
| 65 | Enhanced electrochemical performance of ZnO nanorod core/polypyrrole shell arrays by graphene oxide. Electrochimica Acta, 2016, 187, 517-524. | 5.2 | 38 |
| 66 | p -type conduction in beryllium-implanted hexagonal boron nitride films. Applied Physics Letters, 2009, 95, . | 3.3 | 35 |
| 67 | Accurate Determination of the Index of Refraction of Polymer Blend Films by Spectroscopic Ellipsometry. Journal of Physical Chemistry C, 2010, 114, 15094-15101. | 3.1 | 33 |
| 68 | Annealing of P3HT:PCBM Blend Film—The Effect on Its Optical Properties. ACS Applied Materials & Interfaces, 2013, 5, 4247-4259. | 8.0 | 33 |
| 69 | Fabrication of CuInS ₂ -Sensitized Solar Cells via an Improved SILAR Process and Its Interface Electron Recombination. ACS Applied Materials & Interfaces, 2013, 5, 10605-10613. | 8.0 | 32 |
| 70 | Effect of PTB7 Properties on the Performance of PTB7:PC ₇₁ BM Solar Cells. ACS Applied Materials & Interfaces, 2015, 7, 13198-13207. | 8.0 | 32 |
| 71 | Direct Free Carrier Photogeneration in Single Layer and Stacked Organic Photovoltaic Devices. Advanced Materials, 2017, 29, 1606909. | 21.0 | 32 |
| 72 | Recent progress in cobalt-based carbon materials as oxygen electrocatalysts for zinc-air battery applications. Materials Today Energy, 2021, 20, 100659. | 4.7 | 31 |

| # | Article | IF | CITATIONS |
|----|---|------|-----------|
| 73 | Synthesis and characterization of hard ternary AlMgB composite films prepared by sputter deposition. Thin Solid Films, 2010, 518, 5372-5377. | 1.8 | 30 |
| 74 | Rugated porous Fe3O4 thin films as stable binder-free anode materials for lithium ion batteries. Journal of Materials Chemistry, 2012, 22, 22692. | 6.7 | 30 |
| 75 | Development of a sustainable photocatalytic process for air purification Chemosphere, 2020, 257, 127236. | 8.2 | 29 |
| 76 | Synthesis of CdSXSe1â^'X Nanoribbons with Uniform and Controllable Compositions via Sulfurization: Optical and Electronic Properties Studies. Journal of Physical Chemistry C, 2009, 113, 17183-17188. | 3.1 | 27 |
| 77 | Studying cubic boron nitride by Raman and infrared spectroscopies. Diamond and Related Materials, 2010, 19, 968-971. | 3.9 | 26 |
| 78 | A comparative study on the electronic and optical properties of Sb2Se3 thin film. Semiconductors, 2017, 51, 1615-1624. | 0.5 | 25 |
| 79 | Near field control for enhanced photovoltaic performance and photostability in perovskite solar cells. Nano Energy, 2021, 89, 106388. | 16.0 | 25 |
| 80 | Catalyst-Assisted Formation of Nanocantilever Arrays on ZnS Nanoribbons by Post-Annealing Treatment. Journal of Physical Chemistry B, 2006, 110, 6759-6762. | 2.6 | 24 |
| 81 | Heterocrystal and bicrystal structures of ZnS nanowires synthesized by plasma enhanced chemical vapour deposition. Nanotechnology, 2006, 17, 2913-2917. | 2.6 | 24 |
| 82 | Room-Temperature-Synthesized High-Mobility Transparent Amorphous CdO–Ga ₂ O ₃ Alloys with Widely Tunable Electronic Bands. ACS Applied Materials & Interfaces, 2018, 10, 7239-7247. | 8.0 | 24 |
| 83 | Fluorescent MUA-stabilized Au nanoclusters for sensitive and selective detection of penicillamine. Analytical and Bioanalytical Chemistry, 2018, 410, 2629-2636. | 3.7 | 24 |
| 84 | Improved Nanophotonic Front Contact Design for Highâ€Performance Perovskite Singleâ€Junction and Perovskite/Perovskite Tandem Solar Cells. Solar Rrl, 2021, 5, 2100509. | 5.8 | 23 |
| 85 | Ultraviolet-extended real-time spectroscopic ellipsometry for characterization of phase evolution in BN thin films. Applied Physics Letters, 2001, 78, 1982-1984. | 3.3 | 22 |
| 86 | Luminescent Properties of ZnO Nanorod Arrays Grown on Al:ZnO Buffer Layer. Journal of Physical Chemistry C, 2008, 112, 820-824. | 3.1 | 22 |
| 87 | Characterization of Low-Frequency Excess Noise in CH ₃ NH ₃ PbI ₃ -Based Solar Cells Grown by Solution and Hybrid Chemical Vapor Deposition Techniques. ACS Applied Materials & Interfaces, 2018, 10, 371-380. | 8.0 | 22 |
| 88 | Excitation of Bloch Surface Waves in Zero-Admittance Multilayers for High-Sensitivity Sensor Applications. Physical Review Applied, 2020, 13, . | 3.8 | 22 |
| 89 | Low-temperature treated anatase TiO2 nanophotonic-structured contact design for efficient triple-cation perovskite solar cells. Chemical Engineering Journal, 2021, 426, 131831. | 12.7 | 22 |
| 90 | Aluminium nitride films prepared by reactive magnetron sputtering. Journal Physics D: Applied Physics, 1997, 30, 2147-2155. | 2.8 | 21 |

6

| # | Article | IF | CITATIONS |
|-----|--|---|---|
| 91 | Enhanced Raman scattering from vertical silicon nanowires array. Applied Physics Letters, 2011, 98, 183108. | 3.3 | 21 |
| 92 | Strongly fluorescent cysteamine-coated copper nanoclusters as a fluorescent probe for determination of picric acid. Mikrochimica Acta, 2018, 185, 507. | 5.0 | 21 |
| 93 | Nitrogen-doped silicon nanowires: Synthesis and their blue cathodoluminescence and photoluminescence. Applied Physics Letters, 2009, 95, . | 3.3 | 20 |
| 94 | ZnO-nanorod-array/p-GaN high-performance ultra-violet light emitting devices prepared by simple solution synthesis. Applied Physics Letters, 2012, 101, . | 3.3 | 20 |
| 95 | Materials with extreme properties: Their structuring and applications. Vacuum, 2012, 86, 575-585. | 3.5 | 20 |
| 96 | Ferromagnetism in Ti-doped ZnO thin films. Journal of Applied Physics, 2015, 117, . | 2.5 | 20 |
| 97 | Graphene Oxide–Reduced Graphene Oxide Janus Membrane for Efficient Solar Generation of Water Vapor. ACS Applied Nano Materials, 2021, 4, 1916-1923. | 5.0 | 20 |
| 98 | Stoichiometry Controlled Bipolar Conductivity in Nanocrystalline <mml:math xmlns:mml="http://www.w3.org/1998/Math/MathML" display="inline" overflow="scroll"> <mml:msub> <mml:mi>Ni</mml:mi> <mml:mi>x</mml:mi> <td>>Cd.s/mml +<td>:m19<mml:mi o><mml:mi>Î</mml:mi></mml:mi </td></td></mml:msub></mml:math | >C d.s /mml + <td>:m19<mml:mi o><mml:mi>Î</mml:mi></mml:mi </td> | :m19 <mml:mi o><mml:mi>Î</mml:mi></mml:mi |
| 99 | Physical Review Applied, 2019, 11, . Electrochemical fabrication and optical properties of periodically structured porous Fe2O3 films. Electrochemistry Communications, 2012, 20, 178-181. | 4.7 | 18 |
| 100 | Energy density engineering via zero-admittance domains in all-dielectric stratified materials. Physical Review A, 2018, 97, . | 2.5 | 18 |
| 101 | Ratiometric determination of copper(II) using dually emitting Mn(II)-doped ZnS quantum dots as a fluorescent probe. Mikrochimica Acta, 2018, 185, 511. | 5.0 | 17 |
| 102 | A cubic boron nitride film-based fluorescent sensor for detecting Hg2+. Applied Physics Letters, 2009, 94, . | 3.3 | 16 |
| 103 | Integrated Nanorods and Heterostructure Field Effect Transistors for Gas Sensing. Journal of Physical Chemistry C, 2010, 114, 7999-8004. | 3.1 | 16 |
| 104 | One-pot synthesis of color-tunable copper doped zinc sulfide quantum dots for solid-state lighting devices. Journal of Alloys and Compounds, 2019, 787, 537-542. | 5.5 | 16 |
| 105 | Doubleâ€&ide Crystallization Tuning to Achieve over 1µm Thick and Wellâ€Aligned Block‣ike Narrowâ€&andgap Perovskites for Highâ€Efficiency Nearâ€Infrared Photodetectors. Advanced Functional Materials, 2021, 31, 2010532. | 14.9 | 16 |
| 106 | Electronic structure and optical properties of CdSxSe1â^'x solid solution nanostructures from X-ray absorption near edge structure, X-ray excited optical luminescence, and density functional theory investigations. Journal of Applied Physics, 2014, 116, . | 2.5 | 15 |
| 107 | A generalized Stark effect electromodulation model for extracting excitonic properties in organic semiconductors. Nature Communications, 2019, 10, 5089. | 12.8 | 15 |
| 108 | Infrared organic photovoltaic device based on charge transfer interaction between organic materials. Organic Electronics, 2013, 14, 291-294. | 2.6 | 14 |

| # | Article | IF | CITATIONS |
|-----|---|------|-----------|
| 109 | Composition tuning of room-temperature nanolasers. Vacuum, 2012, 86, 737-741. | 3.5 | 13 |
| 110 | Solution-processable graphene oxide as an insulator layer for metal–insulator–semiconductor silicon solar cells. RSC Advances, 2013, 3, 17918. | 3.6 | 13 |
| 111 | Effect of Temperature, Time, Concentration, Annealing, and Substrates on ZnO Nanorod Arrays Growth by Hydrothermal Process on Hot Plate. Crystallography Reports, 2018, 63, 456-471. | 0.6 | 13 |
| 112 | Electronic structure at the interfaces of vertically aligned zinc oxide nanowires and sensitizing layers in photochemical solar cells. Journal Physics D: Applied Physics, 2011, 44, 325108. | 2.8 | 12 |
| 113 | Metalâ€Free and Metallated Polymers: Properties and Photovoltaic Performance. Macromolecular Chemistry and Physics, 2012, 213, 1300-1310. | 2.2 | 12 |
| 114 | Chemical states and ferromagnetism in heavily Mn-substituted zinc oxide thin films. Journal of Applied Physics, 2014, 115, . | 2.5 | 12 |
| 115 | Multichannel ellipsometry from 1.5 to 6.5 eV for real time characterization of wide band gap materials: phase identification in boron nitride thin films. Diamond and Related Materials, 2001, 10, 1304-1310. | 3.9 | 11 |
| 116 | Evaluation of the biocompatibility and growth inhibition of bacterial biofilms by ZnO, Fe3O4 and ZnO@Fe3O4 photocatalytic magnetic materials. Ceramics International, 2020, 46, 8979-8994. | 4.8 | 11 |
| 117 | Ultralow Thermal Conductivity in Dualâ€Doped nâ€Type Bi ₂ Te ₃ Material for Enhanced Thermoelectric Properties. Advanced Electronic Materials, 2021, 7, 2000910. | 5.1 | 11 |
| 118 | Real-time spectroscopic ellipsometry from 1.5 to 6.5 eV. Thin Solid Films, 2000, 364, 16-21. | 1.8 | 10 |
| 119 | Near-Ultraviolet Light-Emitting Devices Using Vertical ZnO Nanorod Arrays. Journal of Electronic Materials, 2012, 41, 853-856. | 2.2 | 10 |
| 120 | Exploiting nanostructure-thin film interfaces in advanced sensor device configurations. Vacuum, 2012, 86, 757-760. | 3.5 | 10 |
| 121 | Towards FDTD modeling of spectroscopic ellipsometry data at large angles of incidence. Applied Surface Science, 2013, 281, 2-7. | 6.1 | 9 |
| 122 | Surface-Enhanced Emission from Single Semiconductor Nanoribbons. Nano Letters, 2011, 11, 4626-4630. | 9.1 | 8 |
| 123 | On the development of Finite-Difference Time-Domain for modeling the spectroscopic ellipsometry response of 1D periodic structures. Thin Solid Films, 2014, 571, 356-363. | 1.8 | 8 |
| 124 | Construction and Evaluation of High-Quality n-ZnO Nanorod/p-Diamond Heterojunctions. Journal of Nanoscience and Nanotechnology, 2012, 12, 4560-4563. | 0.9 | 7 |
| 125 | Hole-induced large-area homoepitaxial growth of CdSe nanowire arrays for photovoltaic application. Journal of Materials Chemistry A, 2013, 1, 6313. | 10.3 | 6 |
| 126 | Evaluation of the dielectric function of colloidal Cd1â^xHgxTe quantum dot films by spectroscopic ellipsometry. Applied Surface Science, 2017, 421, 295-300. | 6.1 | 6 |

| # | Article | IF | CITATIONS |
|-----|---|------|-----------|
| 127 | Enhanced Light Emission Performance of Mixed Cation Perovskite Films—The Effect of Solution Stoichiometry on Crystallization. Advanced Optical Materials, 2021, 9, 2100393. | 7.3 | 6 |
| 128 | High-quality single-crystal CdSe nanoribbons and their optical properties. Optoelectronics Letters, 2008, 4, 161-164. | 0.8 | 5 |
| 129 | Vertically aligned ZnO nanorods/CdS nanowires branched heterostructures: Cathodoluminescence properties and photovoltaic application. Journal of Crystal Growth, 2013, 374, 65-70. | 1.5 | 5 |
| 130 | The influence of TiO\$_{2}\$ nanostructure properties on the performance of TiO\$_{2}\$-based anodes in lithium ion battery applications. Turkish Journal of Physics, 2014, 38, 442-449. | 1.1 | 5 |
| 131 | Magnetism as a tool for band-gap narrowing of zinc oxide films prepared by sol–gel method. Journal of Sol-Gel Science and Technology, 2016, 77, 240-243. | 2.4 | 5 |
| 132 | Development and Assessment of Nano-Technologies for Cancer Treatment: Cytotoxicity and Hyperthermia Laboratory Studies. Cancer Investigation, 2020, 38, 61-84. | 1.3 | 5 |
| 133 | Enhanced photocatalytic and antifungal activity of ZnO–Cu2+and Ag@ZnO–Cu2+ materials. Ceramics International, 2022, 48, 12660-12674. | 4.8 | 5 |
| 134 | Transmission optimization of multilayer OLED encapsulation based on spectroscopic ellipsometry. Thin Solid Films, 2013, 549, 22-29. | 1.8 | 4 |
| 135 | Convergence and precision characteristics of finite difference time domain method for the analysis of spectroscopic ellipsometry data at oblique incidence. Applied Surface Science, 2017, 421, 878-883. | 6.1 | 4 |
| 136 | A Family of Small Molecular Materials Enabling Consistently Lower Recombination Losses in Organic Photovoltaic Devices. Solar Rrl, 2020, 4, 2000245. | 5.8 | 4 |
| 137 | Influence of annealing temperature on the structural and optical properties of highly-oriented Al and Er co-doped ZnO films. Journal of Materials Science: Materials in Electronics, 2013, 24, 3868-3874. | 2.2 | 3 |
| 138 | Spontaneous Formation of Nanocrystals in Amorphous Matrix: Alternative Pathway to Bright Emission in Quasiâ€2D Perovskites. Advanced Optical Materials, 2019, 7, 1900269. | 7.3 | 3 |
| 139 | Record-high near-band-edge optical nonlinearities and two-level model correction of poled polymers by spectroscopic electromodulation and ellipsometry. Science China Chemistry, 2022, 65, 584-593. | 8.2 | 3 |
| 140 | Solar Cells: Surface Engineering of ZnO Nanostructures for Semiconductorâ€ S ensitized Solar Cells (Adv. Mater. 31/2014). Advanced Materials, 2014, 26, 5575-5575. | 21.0 | 2 |
| 141 | On the modeling of ellipsometry data at large angles of incidence using finite-difference time-domain. Thin Solid Films, 2014, 571, 669-674. | 1.8 | 2 |
| 142 | Characterization of Wide Bandgap Thin Film Growth Using UV-Extended Real Time Spectroscopic Ellipsometry: Applications to Cubic Boron Nitride. Journal of Wide Bandgap Materials, 2002, 9, 191-206. | 0.1 | 0 |
| 143 | Light trapping considerations in self-assembled ZnO nanorod arrays for quantum dot sensitized solar cells. Proceedings of SPIE, 2014, , . | 0.8 | 0 |
| 144 | Ruddlesden–Popper Perovskites: Spontaneous Formation of Nanocrystals in Amorphous Matrix: Alternative Pathway to Bright Emission in Quasiâ€2D Perovskites (Advanced Optical Materials 19/2019). Advanced Optical Materials, 2019, 7, 1970074. | 7.3 | 0 |

IF

ARTICLE All-Dielectric Interference Coating for Sensing Applications. , 2020, , .